MAXIMIZING SIGNAL-TO-NOISE RATIO IN THE RANDOM MUTATION CAPTURE ASSAY

Supplementary Materials

Suresh Kumar Poovathingal[1], Jan Gruber[2], Li Fang Ng[2]
Barry Halliwell[2], Rudiyanto Gunawan[3,*]

[1] Department of Chemical & Biomolecular Engineering, National University of Singapore, 4 Engineering Drive 4, Blk E5 #02-09 Singapore 117576

[2] Department of Biochemistry, Neurobiology and Ageing Program, Centre for Life Science (CeLS), 28 Medical Drive Singapore 117456

[3] Institute for Chemical and Bioengineering, ETH Zürich, HCI F 101, Wolfgang-Pauli-Strasse 10, 8093 Zürich, Switzerland

[*] Author to whom the correspondence should be addressed (**rudi.gunawan@chem.ethz.ch; +41 44 633 21 34 (tel); +41 44 633 12 52 (fax)**).

A Supplementary Text

A.1. Detailed derivation of uncertainty propagation analysis.

The probability of sampling *x* mutant molecules from a well-mixed homogenate into a PCR well can be described using Poisson distribution:

$$P_{Poisson}(x) = \frac{e^{-\lambda}\lambda^{x}}{x!} \qquad x = 0,1,\mathrm{K}\ ,n \tag{1}$$

where λ is the mean number of mutant templates per well. Thus, the probability of sampling zero mutant template into an PCR well, p_0 is simply:

$$p_0 = P_{Poisson}\left(x = 0\right) = e^{-\lambda} \tag{2}$$

Thus, the unknown parameter λ can be estimated from the fraction of wells that are observed to be un-amplified in a given PCR trial as:

$$\hat{\lambda} = -\log \hat{p}_0 \tag{3}$$

where $\hat{p}_0 = n_0 / n_{wells}$ and n_0 and n_{wells} are the number of unamplified and total wells used in the trial, respectively. Since only a small number of n_{wells} is practical, and given that there are but two possible outcomes associated with each PCR wells (either the well is amplified due to the presence of DNA template or the well remains unamplified), the number n_0 follows a Binomial distribution with a probability given by:

$$P\left(n_0\right) = \begin{pmatrix} n_{wells} \\ n_0 \end{pmatrix} p_0^{n_0} \left(1 - p_0\right)^{n_{wells} - n_0}. \tag{4}$$

From the properties of Binomial distribution, we know that the random number n_0 has a mean of $n_{wells}p_0$ and a variance of $n_{wells}p_0(1-p_0)$, which translate to a mean and variance of $\hat{p}_0$ (observed) of p_0 (actual) and $p_0(1-p_0)/n_{wells}$, respectively.

The uncertainty analysis of $\hat{\lambda}$ relies on a first order linear approximation, in which the variance of any function of random variables, $y=g(x)$ is approximated from a Taylor Series Expansion (TSE) about the estimator for the mean of the random variables *x*, given by

$$V(y) \approx \sum_{\mathbf{x}} \left(\left. \frac{\partial g}{\partial x} \right|_{x=\hat{x}} \right)^2 V(x) \tag{5}$$

where $\hat{x}$ is an unbiased estimator of the mean of *x*. Since $\hat{p}_0$ is an unbiased estimate for p_0, the uncertainty in the estimate $\hat{\lambda}$ or $V(\hat{\lambda})$ can be obtained as a function of the uncertainty in $\hat{p}_0$ according to:

$$\begin{aligned} V(\hat{\lambda}) &\approx \left(\left. \frac{\partial(-\log p_0)}{\partial p_0} \right|_{p_0=\hat{p}_0} \right)^2 V(\hat{p}_0) \\ V(\hat{\lambda}) &\approx \left(\frac{1}{\hat{p}_0} \right)^2 \frac{\hat{p}_0(1-\hat{p}_0)}{n_{wells}} \\ V(\hat{\lambda}) &\approx \frac{1-\hat{p}_0}{n_{wells}\hat{p}_0} \end{aligned} \tag{6}$$

The coefficient of variation (CV) for the above function thus becomes

$$CV(\hat{\lambda}) \approx \frac{1}{-\log(\hat{p}_0)} \sqrt{\frac{1-\hat{p}_0}{n_{wells}\hat{p}_0}} \tag{7}$$

The CV from the linearized analysis above has a minimum inflection at about $p_0 \approx 0.2$, which is in agreement with the Monte Carlo simulations below (**Supplementary Fig. 1A** and **Figure. 2A** in the **main text**).

The mutation frequency estimate $\hat{\theta}$ (mutant per base pair) can then be calculated from $\hat{\lambda}$ according to:

$$\hat{\theta} = \frac{\hat{\lambda}}{n_{bp} n_{mtDNA}} \tag{8}$$

where n_{mtDNA} is the total number of mtDNA in a single PCR well and n_{bp} is the length DNA template in consideration (in base pairs; e.g., n_{bp} = 4 for *Taq*I recognition site (7)).

A.2. Pseudo-codes for Monte Carlo Simulations

A.2.1. Pseudo-code for the sampling protocol in the original RMC assay

Steps **Algorithm**

1 Initialization

set the number of PCR wells n_{wells}

set frequencies of false positive(α) and false negatives(β) errors

seed random number generators (both uniform and non-uniform)

set template copy number n_{mtDNA}

set the iteration counter to $k \Rightarrow 0$

2 Iterations

while $k \leq 10000\,(I_{tot})$

initialize the counter for amplified wells $i_A \Rightarrow 0$

set counter for number of wells per PCR plate $n \Rightarrow 1$

while $n \leq n_{wells}$

generate a Uniform random number $U(0,1) : r$

generate a Binomial or Poisson (depending on the case) random number $B(n,\theta)$ or $P(\lambda) \Rightarrow R$

if $R \neq 0$, then:

if $r \geq \beta$, then:

$i_A = i_A + 1$

else

if $r < \alpha$, then:

$i_A = i_A + 1$

increment $n+1$

calculate the estimate of mutation frequency

$$\hat{\theta} = \frac{i_A}{n_d \times n_{well}}$$

increment $k+1$

A.1.2. Pseudo-code for the sampling protocol in the optimized RMC assay

Steps	Algorithm
1	**Initialization**
	set the number of PCR wells n_{wells}
	set frequencies of false positive(α) and false negatives(β) errors
	seed random number generators (both uniform and non-uniform)
	set mean fraction of unamplified well(p_0)
	If using Binomial case, set number of mtDNA in a PCR well (n_{mtDNA})
	set the iteration counter to $k \Rightarrow 0$
2	**Iteration**
	while $k \le 10000 (I_{tot})$
	set the counter for unamplified wells $i_{UA} \Rightarrow 0$
	set counter for number of wells per PCR plate $n \Rightarrow 1$
	while $n \le n_{wells}$
	generate a Uniform random number $U(0,1) : r$
	generate a Binomial or Poisson (depending on the case) random number $B(n,\theta)$ or $P(\lambda) \Rightarrow R$
	if $R = 0$, then:
	if $r \ge \alpha$, then:
	$i_{UA} = i_{UA} + 1$
	else
	if $r < \beta$, then:
	$i_{UA} = i_{UA} + 1$
	increment n+1
	calculate the fraction of unamplified wells $\hat{p}_0 = \frac{i_{UA}}{n_{wells}}$
	calculate the estimate of mutation frequency $\hat{\theta}$
	increment $k+1$

A.3. Simulation Methodology

Following our mtDNA point mutation model (26), the *in silico* model developed in this work, tracks for mtDNA mutation accumulation during two stages: developmental and postnatal (Figure TXT1). The model comprises of tracking the wild-type mtDNA (*W*) and mtDNA deletion (*M*) in each cardiomyocytes of the mouse heart tissue (25×10^6cells). Each mutant mtDNA molecule is assumed to contain only a single mutation in the *Taq*I recognition site (TCGA), consistent with the RMC experimental design (7). The probability of finding two or more mutations at the same site is negligible (3). In the subsequent section, details of the stochastic model used in this work for the CME representation of mitochondrial turnover process will be discussed.

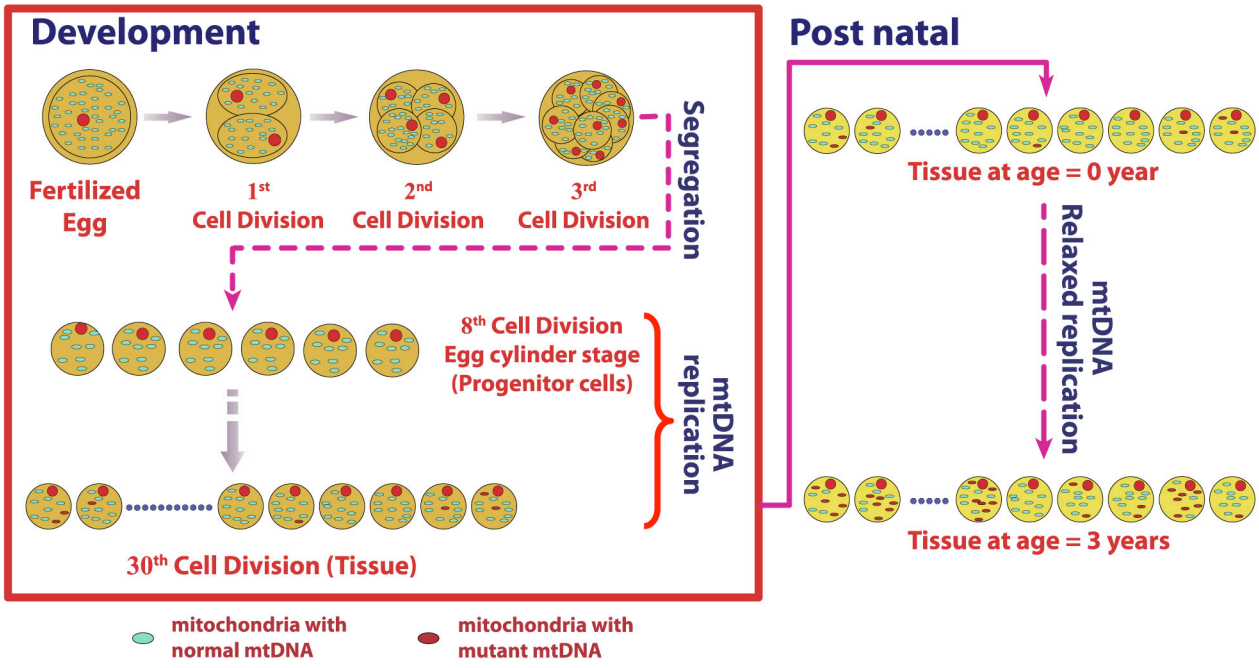

Figure TXT1: Stochastic model of mtDNA turnover process in mouse heart tissue. The *in silico* mouse model simulates the point mutation load of mtDNA in all the cells of mouse heart tissue during development and postnatal stages.

A.3.1. Cell-level modeling details

Based on experimental evidence, each mitochondrion is assumed to contain 10 mtDNA organized into assemblies called nucleoids (28,29). The model simulates two mtDNA-related maintenance processes: mitochondrial turnover comprising of relaxed replication and degradation of mtDNA, and *de novo* point mutations arising during mtDNA replication (Figure TXT2). The model is based on a minimal conservative assumption of the cellular mtDNA population existing as a well-mixed pool, due to fast fusion and fission dynamics of mitochondria (30). Analysis of mtDNA replication process using labeling kinetics have indicated that all genome replicate independent from each other and also the independence is conserved at the level of nucleoids (28). Consistent with these observations, in a turnover event, each mitochondrial DNA is randomly sampled and subjected to replication. Each mitochondrion that undergoes autophagy (or mitophagy) is assumed to contain random number of mtDNA copy number (n_{mito}), sampled according to Poisson distribution (with mean mtDNA count = 10) (27,28), and the number of wild-type mtDNA undergoing degradation is obtained as:

$$f(x) = \frac{\binom{W}{x}\binom{M}{n_{mito}-x}}{\binom{W+M}{n_{mito}}} \qquad [9]$$

where x represents the number of wild type mtDNA chosen for the mitophagy.

De novo point mutation can occur during replication of mtDNA due to mis-pairing associated with ROS-induced mutagenic lesions such as 8-hydroxy-2-deoxyguanosine (8OHdG)

(31) or as random errors arising due to finite polymerase-γ (POLG) fidelity (32). Consequently, each replication of a wild-type mtDNA has a finite probability, given by the mutation rate constant (k_m), to produce a mutant. In a mutation event, single mutated mtDNA forms and the original mtDNA molecule remains intact. Thus, in the event of a *de novo* point mutation, mutant mtDNA count is increased and the wild-type mtDNA population is conserved. Here, the number of *de novo* mutant mtDNA is randomly chosen from a binomial distribution: (27)

$$g(y) = \binom{x}{y} \cdot k_m^{y} \cdot (1-k_m)^{x-y} \qquad [10]$$

where *y* denotes the number of *de novo* mutations resulting from replication of *x* wild-type mtDNA.

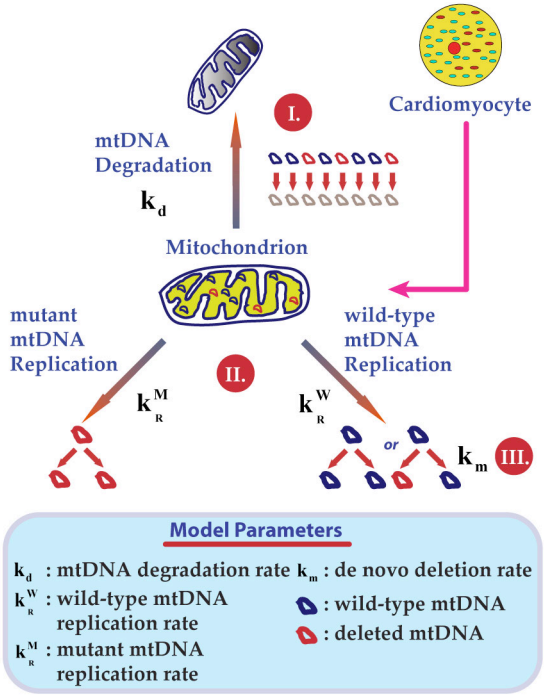

Figure TXT2: Stochastic model of mtDNA turnover dynamics in a mouse cardiomyocytes. Stochastic drift in mtDNA deletion dynamics results from following random processes. (I) The mitochondrion that undergoes a

turnover event is randomly selected from the population. The autophagy of mitochondrion is simulated by removing all the mtDNA molecules associated with the mitochondrion. (II) Replication of a single mtDNA molecule occurs by random selection of mtDNA from the mitochondrial DNA population. (III) During the wild-type mtDNA replication, there exists a finite probability equal to the *de novo* mutation rate (k_m) for the replication process to give a mutant mtDNA.

Based on these probabilities, the *in silico* model is formulated as Chemical Master Equation (CME) (33) in which each mtDNA-related process: replication without mutation, replication with *de novo* mutations and degradation, is described as a jump Markov process with the following state transitions (Figure TXT2):

$$\begin{aligned} W &\xrightarrow{k_d} \phi \\ M &\xrightarrow{k_d} \phi \\ W &\xrightarrow{(1-k_m)\cdot k_R} W + W \\ M &\xrightarrow{k_R} M + M \\ W &\xrightarrow{k_m \cdot k_R} W + M \end{aligned} \qquad [11]$$

The first two transitions reflect the mitochondrial degradation (mitophagy), the third and forth reactions represent replication of mtDNA without mutation, and the last reaction represents the *de novo* mtDNA point mutation. A general formulation of CME for the mtDNA turnover process is given by (26,34):

$$
\begin{aligned}
\frac{\partial P(W,M;t)}{\partial t} = \; & k_d \cdot \sum_{x=0}^{10} \left\{ \frac{\binom{W+x}{x}\binom{M+(10-x)}{10-x}}{\binom{W+M+10}{10}} \right\} \cdot \left(W+x+M+(10-x)\right) \\
& \cdot P\left(W+x, M+(10-x); t\right) \\
& - k_d \cdot \sum_{x=0}^{10} \left\{ \frac{\binom{W}{x}\binom{M}{10-x}}{\binom{W+M}{10}} \right\} \cdot (W+M) \cdot P(W,M;t) \\
& + k_m \cdot k_R \cdot P(W, M-1; t) - k_m \cdot k_R \cdot P(W,M;t) \\
& + (1-k_m) \cdot k_R \cdot P(W-1, M; t) - (1-k_m) \cdot k_R \cdot P(W,M;t) \\
& + k_R \cdot P(W, M-1; t) - k_R \cdot P(W,M;t)
\end{aligned}
\qquad [12]
$$

The probability density function $P(W,M;t)$ denotes the probability of a cell in a tissue to contain W and M copy numbers of wild-type and mutated mtDNA, respectively, given an initial condition of the mtDNA population in the cell ($P\left(W,M;t\middle|W_0,M_0\right)$, not explicitly stated here for brevity). The parameters k_d, k_m and k_R are the specific probability rate constants of mtDNA degradation, *de novo* mutations and replication rates, respectively. The terms in the curly braces of Equation 4 represent the hypergeometric sampling of mtDNA from the mitochondrial population. The first two terms in Equation 4 represents degradation of mtDNA in a single mitochondrion. The third line in the Equation 4 represents the *de novo* deletion generated during the replication of a wild-type mtDNA. The last pair of terms corresponds to replication of wild-type and mutant mtDNA. The CME can be solved numerically using a Monte Carlo approach following modified Stochastic Simulation Algorithm (SSA) (33,35). The implementation of the modified SSA is described below:

1. Compute the propensities of replication and degradation processes as a function of *W* and *M* at time *t*.
2. Based on the propensities, generate random samples of (τ, *j*) as in the SSA algorithm (33,35).
3. Select ten mtDNA molecules randomly from the population (hypergeometric sampling) for mitochondrial degradation and similarly select a single mtDNA from the population for the process of replication. Each replication of a wild type mtDNA can result in a mutant mtDNA with a probability given by the mutation rate constant (k_m).
4. Update *W* and *M* based on events in steps 2 and 3 and increment the time *t* by τ.
5. Repeat steps 1 through 4 until the desired end time.

To predict mtDNA mutation burden in a single organ or tissue, millions of such simulations are performed to capture the mtDNA dynamics of all cells in a tissue.

A.3.2. Tissue-level modeling details

A.3.2.1. Simulations of mouse development

The developmental simulation not only captures the rapid increase in cell number and the associated increase in the mtDNA copy number in the developmental embryonic cells, but also accounts for the normal turnover of mtDNA. The embryonic cell divisions begin after fertilization of an oocyte. Mouse oocytes harbor a large number of mitochondria (~1.5×10^5 mtDNA) (36), which allow the zygote to multiply initially without the need to replicate mtDNA (37,38). Furthermore, the total mtDNA number in mouse embryo does not increase until the late stage of

blastocyst, which is roughly the 7^{th} to 8^{th} cell divisions in development (i.e., 4.7 to 5.5 days post coitum (d.p.c)) (37-39). During these stages, mtDNA are segregated among the dividing progenitor cells (Figure TXT1). Consequently, each progenitor cell of the developing embryo has only few copies of mtDNA at the early egg-cylinder stage (37,38).

In order to account for the mtDNA segregation without replication during the initial cell divisions, the developmental simulations start from the end of the 8^{th} stage (5 d.p.c) with an initial mtDNA copy number of ~1000 mtDNA in the embryonic cells during the mouse embryogenesis (W = 1000, M = 0) (40). Mitochondrial DNA replication is tied to the cellular division to maintain a steady state number of total mtDNA after each division (41). Mouse development lasts until 20 d.p.c (42) with a doubling time of roughly 15.5 hours (43). The mtDNA replication rate is estimated assuming that mtDNA doubles its population every 15 hours while still undergoing degradation. Here, a cell division occurs when the total number of mtDNA count reaches roughly twice the steady state homeostatic count (Table TXT1). The segregation of wild-type and mutant mtDNA between the daughter cells is assumed to occur at random, without any selective advantage according to a hypergeometric distribution: (27)

$$f(x) = \frac{\binom{W}{x}\binom{M}{n-x}}{\binom{W+M}{n}} \qquad [13]$$

where x denotes the number of wild-type mtDNA in one of the daughter cells after segregation and n is the total number of mtDNA in a single daughter cell (i.e., $n = (W+M)/2$). During

development, POLG the care taker of the mtDNA replication fidelity, is the main contributor for point mutations in mtDNA, with negligible oxidative activity and damage (32,44).

A.3.2.2. Simulations of postnatal stage

After birth, cardiomyocytes do not undergo further cellular division. However, the mtDNA population in cardiomyocytes undergoes hypertrophic growth. The mtDNA population in the mouse cardiomyocytes increases from 1000 molecules to ~3500 copies per cell (45-47). After reaching the nominal count of mtDNA in adult cardiomyocytes (47), the mtDNA copy number of cardiomyocytes is held at constant level, by relaxed replication (48). The functional significance of relaxed replication in postmitotic tissues like heart and brain is to maintain a healthy population of mtDNA to satisfy the cellular energy requirements (48,49). The postmitotic simulations continue from cells produced at the last stage of development (Figure TXT1), in which each cell maintains mitochondrial biogenesis to balance degradation. Like the developmental stage, the POLG replication fidelity is assumed to be the main contributor for point mutations in mtDNA, with negligible oxidative activity and damage.

A.3.2.3. Calculation of mtDNA point mutation frequency

The point mutation burden (mutation frequency) per base pair is determined using,

$$\Delta_f^{sim} = \frac{M_{tot}}{\left(W_{tot} + M_{tot}\right) \cdot 4bp} \qquad [14]$$

where W_{tot} and M_{tot} are the total number of wild-type and mutant mtDNA molecules in the tissue, respectively. Consistent with the original work, the length of *Taq*I recognition site used in

the RMC assay is 4 bp (7). Note, that the probability of a molecule with two or more mutations in the same *Taq*I site is negligible (7).

All simulations were performed using an IBM high performance computing cluster with ~140 Intel 1.6 GHz processors. The simulations were coded and compiled using GNU C++ compiler; G++ (v4.1.1) and run on CentOS (RHEL) Linux platform. On average a complete simulation of a heart tissue (~20 million cells) from the development to the end of 3 years of mouse's life span required approximately 7 hours.

A.3.3. Model Parameters

Model parameters are compiled from published data for mice and we have ensured that they are consistent with the current literature and the state of the art techniques. The model parameters used in this work is listed in Tables TXT1.

A.3.3.1. Mitochondrial DNA degradation rate (k_d)

Cellular organelles like mitochondria are normally degraded by the autophagy process, where an entire organelle is engulfed by a lysosome and undergone lytic degradation (50). Different half lives obtained using different methods and based on different reference macromolecules are simulated to compare the effect of different mitochondrial turnover rates on the resulting mtDNA mutation accumulation dynamics in cells of postmitotic tissue.

A.3.3.2. Mitochondrial DNA replication rate (k_R)

The mtDNA copy number is maintained throughout the cell growth and divisions (51). The mtDNA replication should occur to balance the degradation. We have used a constant biogenesis model

to simulate the mtDNA replication process. The constant mtDNA replication rate was deduced based on the homeostatic mtDNA copy number in a cell and the degradation rate of mtDNA. Thus, the replication constant k_R is given by:

$$k_R = k_d \cdot (W + M)_{ss} \quad [15]$$

A.3.3.3. Mitochondrial DNA point mutation rate (k_m)

The fidelity of polymerase-γ contributes to *de novo* point mutations during replication. The polymerase is responsible for the replication and proof reading of newly synthesized strands with a reported error rate between 1×10^{-7} and 1×10^{-6} bp^{-1}replication^{-1} for the wild-type enzyme (32). A conservative value (lowest) of 1×10^{-7} bp^{-1} replication^{-1} is chosen for wild-type mouse simulations.

All the other model parameters are consistent with our earlier work (26) and the model parameters are compiled from the published data on mice and we have ensured to select parameters that are consistent with the current literature and the state of the art measurement techniques. The summary of all the parameters used in this work is described in Table TXT1.

Table TXT1 : Model parameters of the stochastic mtDNA turnover process in the cardiomyocytes of *in silico* wild-type mouse model

Rates	Unit	Values	Comments	References
W_0	*molecules*	1000	Initial value of wild type mtDNA during start of development	(37,38,40)
M_0	*molecules*	0	Initial value of mutant mtDNA during start of development	
k_d	d^{-1}	2.3377×10^{-3}	Degradation rate of mtDNA	(52)
$\nu_R^{\max}\big\|_{dev}$	*molecules* d^{-1}	5567.85	Maximum replication rate of mtDNA during development	
$\nu_R^{\max}\big\|_{PN}$	*molecules* d^{-1}	8.18195	Maximum replication rate of mtDNA during post natal stage	
N_{cyc}	-	22	Number of developmental cycles	(39,42,43,53)
$(W+M)_{ss}$	*molecules*	3500	Homeostatic set-point of the mtDNA population (skeletal muscle)	(47)
k_m	rep^{-1}	4×10^{-7}	*de novo* deletion rate of mtDNA	(32,44,54)
N_{cell}	-	2.2443×10^{7}	Number of myoblast at development	(47,55)

References

3. Bielas, J.H. and Loeb, L.A. (2005) Quantification of random genomic mutations. *Nat Methods*, **2**, 285-290.
7. Vermulst, M., Bielas, J.H., Kujoth, G.C., Ladiges, W.C., Rabinovitch, P.S., Prolla, T.A. and Loeb, L.A. (2007) Mitochondrial point mutations do not limit the natural lifespan of mice. *Nat Genet*, **39**, 540-543.
26. Poovathingal, S.K., Gruber, J., Halliwell, B. and Gunawan, R. (2009) Stochastic drift in mitochondrial DNA point mutations: a novel perspective ex silico. *PLoS Comput Biol*, **5**, e1000572.
27. Montgomery, D.C. and Runger, G.C. (2006) *Applied Statistics and Probability for Engineers*. Wiley, New York.
28. Iborra, F.J., Kimura, H. and Cook, P.R. (2004) The functional organization of mitochondrial genomes in human cells. *BMC Biol*, **2**, 9.
29. Satoh, M. and Kuroiwa, T. (1991) Organization of multiple nucleoids and DNA molecules in mitochondria of a human cell. *Exp Cell Res*, **196**, 137-140.
30. Chen, H. and Chan, D.C. (2005) Emerging functions of mammalian mitochondrial fusion and fission. *Hum Mol Genet*, **14 Spec No. 2**, R283--R289.
31. Halliwell, B. and Aruoma, O.I. (1991) DNA damage by oxygen-derived species. Its mechanism and measurement in mammalian systems. *FEBS lett*, **281(1-2)**, 9--19.
32. Kunkel, T.A. (1992) DNA Replication Fidelity. *J Biol Chem*, **267(26)**, 18251--18254.
33. Gillespie, D.T. (1991) *Markov Processes: An Introduction for Physical Scientists*. Academic Press, San Diego.
34. Gardiner, C.W. (2004) *Handbook of Stochastic Methods: for Physics, Chemistry and the Natural Sciences (Springer Series in Synergetics)*. Springer, Berlin.
35. Gillespie, D.T. (1977) Exact Stochastic Simulation of Coupled Chemical Reactions. *J Phys Chem*, **81**, 2340--2361.
36. Steuerwald, N., Barritt, J.A., Adler, R., Malter, H., Schimmel, T., Cohen, J. and Brenner, C.A. (2000) Quantification of mtDNA in single oocytes, polar bodies and subcellular components by real-time rapid cycle fluorescence monitored PCR. *Zygote*, **8**, 209--215.
37. Elliott, K. and O'Connor, M. (1976) *Embryogenesis in mammals (Ciba Foundation symposium ; 40)*. Elsevier.
38. Piko, L. and Taylor, K.D. (1987) Amounts of mitochondrial DNA and abundance of some mitochondrial gene transcripts in early mouse embryos. *Dev Biol*, **123**, 364--374.
39. Larsson, N.G., Wang, J., Wilhelmsson, H., Oldfors, A., Rustin, P., Lewandoski, M., Barsh, G.S. and Clayton, D.A. (1998) Mitochondrial transcription factor A is necessary for mtDNA maintenance and embryogenesis in mice. *Nat Genet*, **18**, 231--236.
40. Cao, L., Shitara, H., Horii, T., Nagao, Y., Imai, H., Abe, K., Hara, T., Hayashi, J. and Yonekawa, H. (2007) The mitochondrial bottleneck occurs without reduction of mtDNA content in female mouse germ cells. *Nat Genet*, **39**, 386-390.
41. Moraes, C.T. (2001) What regulates mitochondrial DNA copy number in animal cells? *Trends Genet*, **17(4)**, 199--205.
42. Sissman, N.J. (1970) Developmental Landmarks in Cardiac Morphogenesis: Comparative Chronology. *Am J Cardiol*, **25**, 141--148.
43. Karatza, C., Stein, W.D. and Shall, S. (1984) Kinetics of in vitro ageing of mouse embryo fibroblasts. *J Cell Sci*, **65**, 163--175.

44. Cervantes, R.B., Stringer, J.R., Shao, C., Tischfield, J.A. and Stambrook, P.J. (2002) Embryonic stem cells and somatic cells differ in mutation frequency and type. *Proc Natl Acad Sci USA*, **99(6)**, 3586--3590.
45. Dubec, S.J., Aurora, R. and Zassenhaus, H.P. (2008) Mitochondrial DNA mutations may contribute to aging via cell death caused by peptides that induce cytochrome c release. *Rejuvenation Res*, **11**, 611-619.
46. Miller, F.J., Rosenfeldt, F.L., Zhang, C., Linnane, A.W. and Nagley, P. (2003) Precise determination of mitochondrial DNA copy number in human skeletal and cardiac muscle by a PCR-based assay: lack of change of copy number with age. *Nucleic Acids Res*, **31**, e61.
47. Wiesner, R.J., Ruegg, J.C. and Morano, I. (1992) Counting target molecules by exponential polymerase chain reaction: copy number of mitochondrial DNA in rat tissue. *Biochem. Bioph. Res. Co.*, **183(2)**, 553--559.
48. Clayton, D.A. (1982) Replication of animal mitochondrial DNA. *Cell*, **28**, 693--705.
49. Shadel, G.S. and Clayton, D.A. (1997) Mitochondrial DNA Maintenance in vertebrates. *Ann Rev Biochem*, **66**, 409--435.
50. Terman, A. and Brunk, U.T. (2005) Autophagy in cardiac myocyte homeostasis, aging, and pathology. *Cardiovasc Res*, **68**, 355--365.
51. Davis, A.F. and Clayton, D.A. (1996) In Situ Localization of Mitochondrial DNA Replication in Intact Mammalian Cells. *J Cell Biol*, **135**, 883--893.
52. Collins, M.L., Eng, S., Hoh, R. and Hellerstein, M.K. (2003) Measurement of mitochondrial DNA synthesis in vivo using a stable isotope-mass spectrometric technique. *J Appl Physiol*, **94**, 2203-2211.
53. Taylor, R.W. and Turnbull, D.M. (2005) Mitochondrial DNA mutations in human disease. *Nat Rev Genet*, **6**, 389-402.
54. Zhang, D., Mott, J.L., Chang, S.W., Denniger, G., Feng, Z. and Zassenhaus, H.P. (2000) Construction of transgenic mice with tissue-specific acceleration of mitochondrial DNA mutagenesis. *Genomics*, **69**, 151-161.
55. Limson, M. and Jackson, C.M. (1931) Changes in the weights of various organs and systems of young rats maintained on a low-protein diet. *J Nutr*, **5(2)**, 163--174

B. SUPPLEMENTARY FIGURES

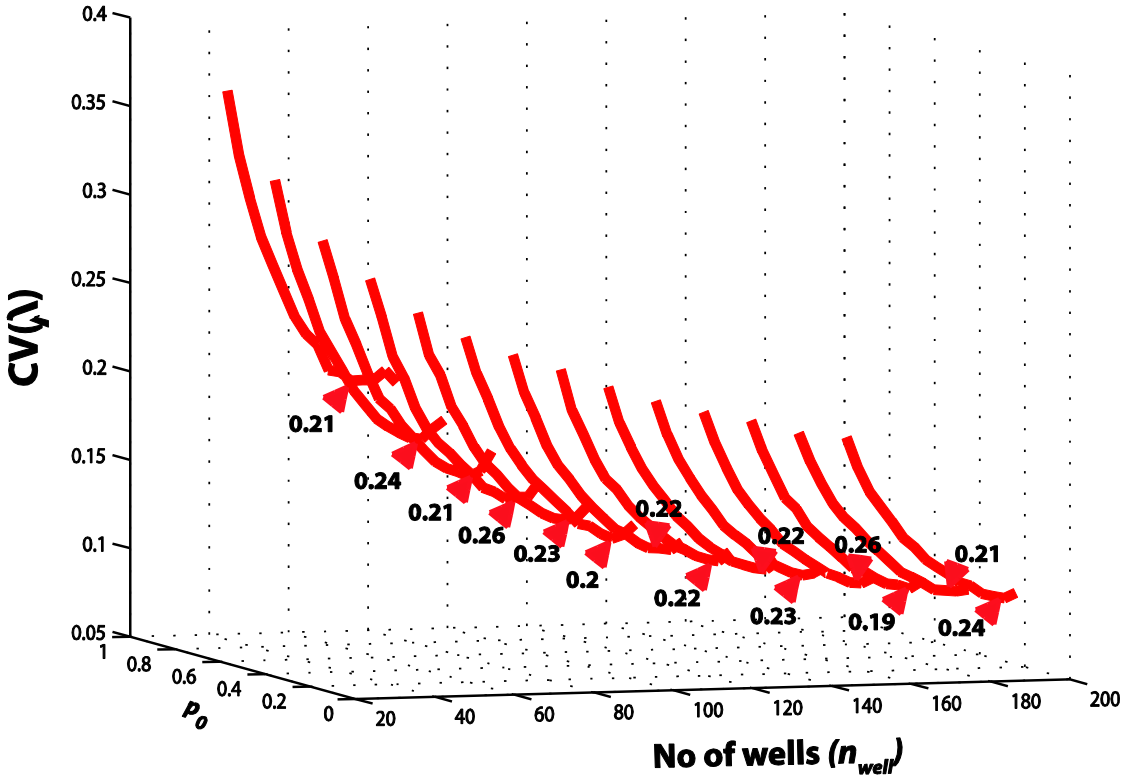

Supplementary Figure. 1: Coefficient of Variation (CV) obtained using Poisson statistics as a function of the fractions of unamplified wells (p_0) and the total number of PCR wells (n_{wells}), determined using Monte Carlo simulations. The arrows indicate the minimum value of CVs. The optimal value of p_0 mostly ranged between 0.2 and 0.3.

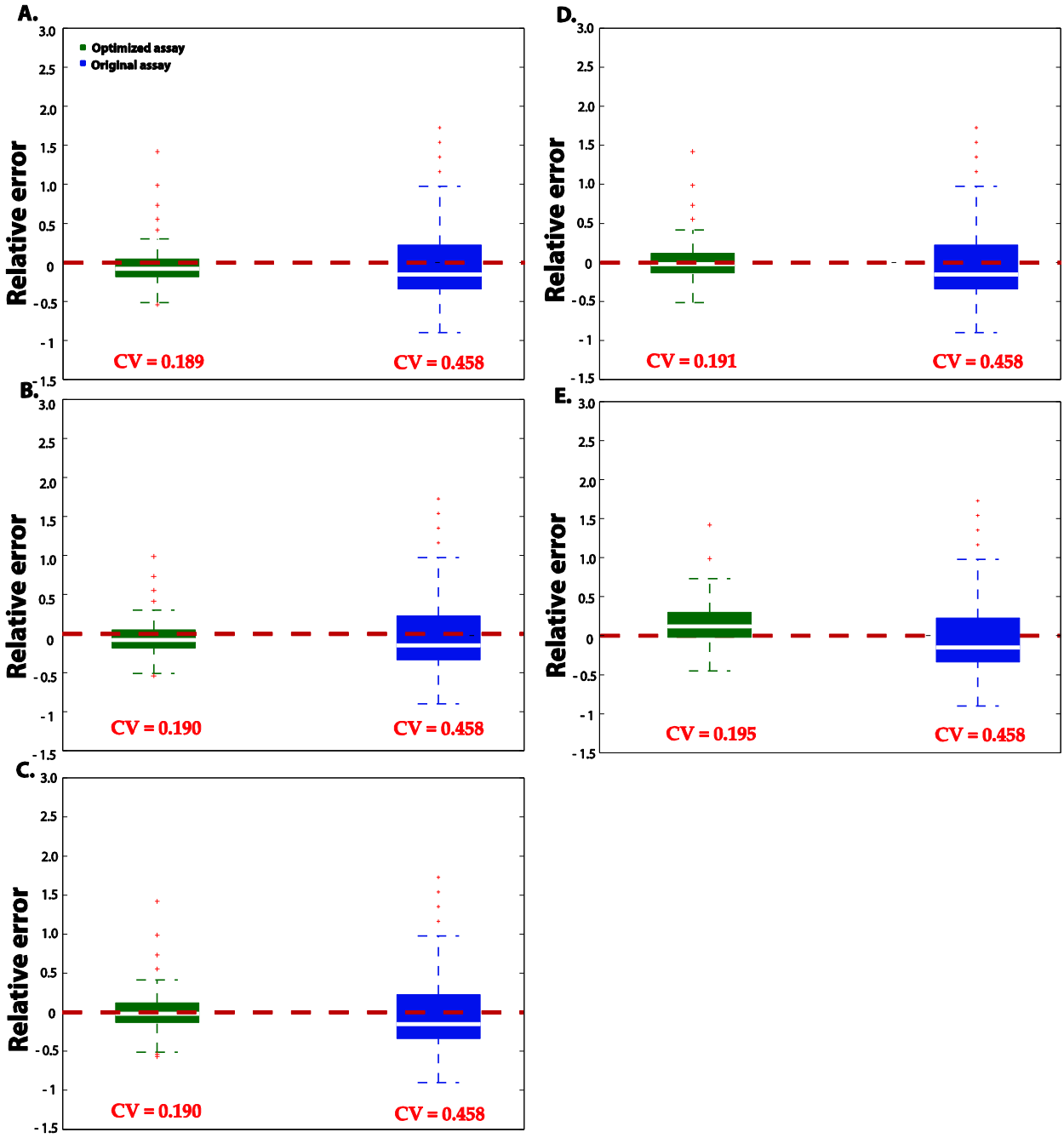

Supplementary Figure 2: Influence of type – I error (false amplification) on the performance of the proposed RMC protocol. The relative differences between $\hat{\lambda}$ and the true value λ were obtained from 10^4 MC independent realizations. The true λs were 1.6 and 0.1 molecules per well for the optimized and the conventional RMC assay, respectively. In the conventional RMC assay, type-I error is assumed to be zero. In both assays, the error rate of type – II (false non-amplification) is set at 4% based on experimental data (**Supporting Table 1**). Type- I error rates used in the simulations of the proposed RMC protocol were: A.) 2%, B.) 4%, C.) 8%, D.) 15% and E.) 30%.

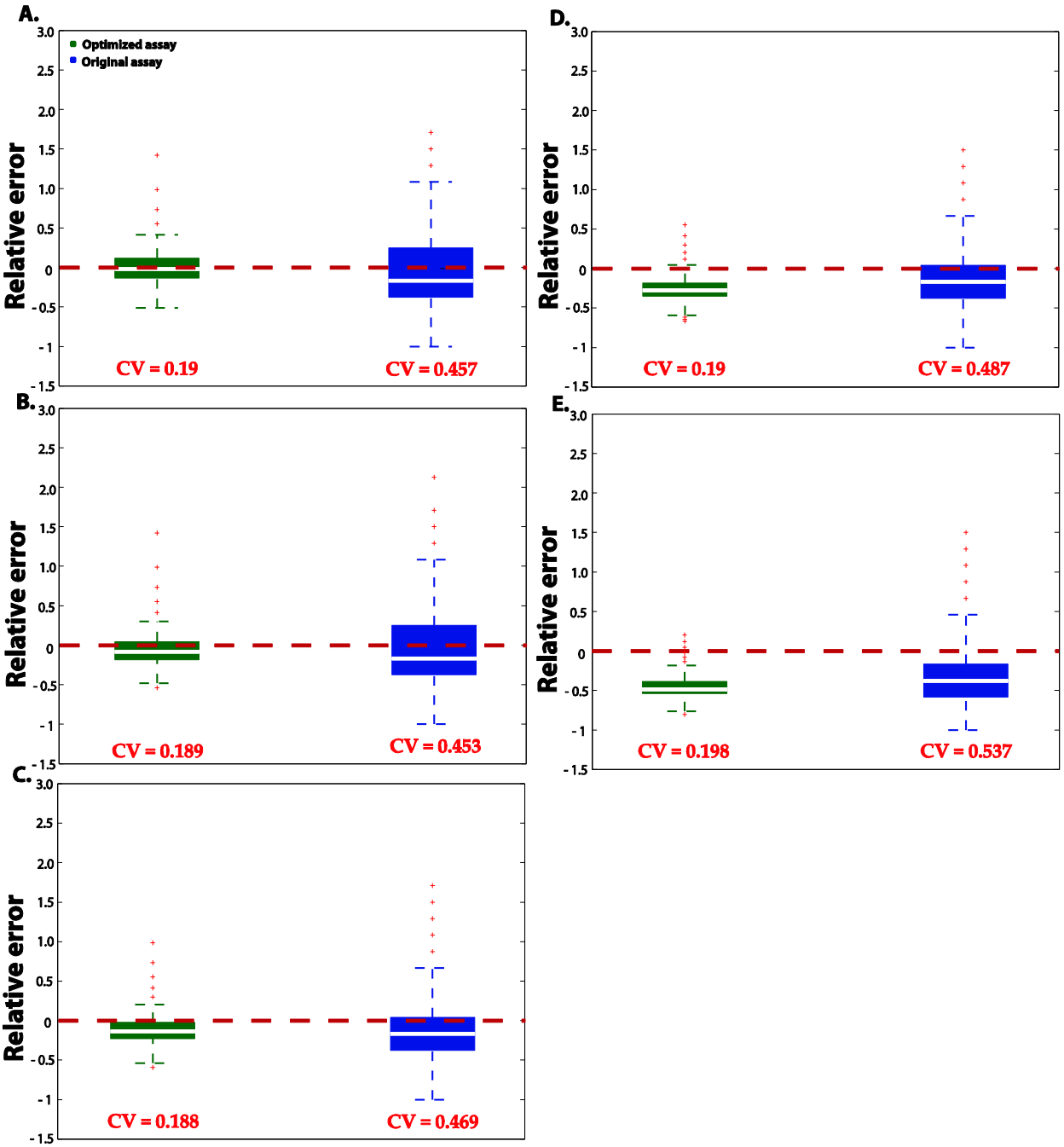

Supplementary Figure 3: Influence of type – II error (false non-amplification) on the performance of the optimized and original RMC protocol. The relative differences between $\hat{\lambda}$ and the true value λ were obtained from 10^4 MC independent realizations. The true λs were 1.6 and 0.1 molecules per well for the optimized and the conventional RMC assay, respectively. In the conventional RMC assay, type-I error is assumed to be zero. The frequency of type-I error (false amplification) for the optimized RMC was set at 6% based on experimental data (**Supporting Table. 1**). Type- II rates used for simulations of both the conventional RMC assay and the proposed optimal RMC assay were: A.) 2%, B.) 4%, C.) 8%, D.) 15% and E.) 30%.

C. SUPPLEMENTARY TABLES

Supplementary Table 1: Frequencies of false positives and false negatives encountered during the RMC trials. Data is based on the quality control experiments of the RMC assay conducted using the NTC's and mtDNA templates. Trials used for obtaining the false positive error frequencies were conducted with PCR amplification of the wells having pure buffer (NTC's). Whereas, the trails used for determining the false negative error frequencies were based on amplification of the PCR wells with an average of 10 mtDNA templates in each of the PCR wells.

Thermal Cycler Profile

Stage	Repetitions	Temperature	Time	Ramp Rate
1	1	50.0 °C	2:00	100
2	1	95.0 °C	10:00	100
3	70	95.0 °C	0:45	100
		55.0 °C	0:45	100
		72.0 °C	1:30	100

Standard 7500 Mode
Data Collection : Stage 3 Step 3
PCR Volume: 20 µL

Type - I error	
Number of wells used for the trial	100
Number of wells amplified	6
Error frequency	**6%**
Type - II error	
Number of wells used for the trial	100
Number of wells amplified	96
Error frequency	**4%**

Supplementary Table 2: Citations related to the direct application of RMC assay, since its inception. (source: Pubmed)

Studies using the RMC method:

	Year of Publication	Author	Article	Journal	Volume	Issue	Page No.	Impact Factor (JCR 2009)
1	2011	Biniecka, M. *et al.*	Successful tumour necrosis factor (TNF) blocking therapy suppresses oxidative stress and hypoxia-induced mitochondrial mutagenesis in inflammatory arthritis.	Arthritis Research and Therapy	Epub ahead of print			4.36
2	2011	Biniecka, M. *et al.*	Hypoxia induces mitochondrial mutagenesis and dysfunction in inflammatory arthritis.	Arthritis and Rheumatism	Epub ahead of print			7.332
3	2011	Wright, J.H. *et al.*	A random mutation capture assay to detect genomic point mutations in mouse tissue.	Nucleic Acids Research	39	11	E73	7.479
4	2010	Gorman, S. *et al.*	Mitochondrial mutagenesis induced by tumor-specific radiation bystander effects.	Journal of Molecular Medicine	88	7	701-8	5.004
5	2010	Chen, H. *et al.*	Mitochondrial fusion is required for mtDNA stability in skeletal muscle and tolerance of mtDNA mutations.	Cell	141	2	280-9	31.152
6	2010	Dai, D.F. *et al.*	Age-dependent cardiomyopathy in mitochondrial mutator mice is attenuated by overexpression of catalase targeted to mitochondria.	Aging Cell	9	4	536-44	7.554
7	2009	Dai, D.F. *et al.*	Overexpression of catalase targeted to mitochondria attenuates murine cardiac aging.	Circulation	119	21	2789-97	14.816
8	2009	Greaves, L.C. *et al.*	Quantification of mitochondrial DNA mutation load.	Aging Cell	8	5	566-72	7.554
9	2008	Vermulst, M. *et al.*	Quantification of random mutations in the mitochondrial genome.	Methods	46	4	263-8	3.763
10	2008	Vermulst, M. *et al.*	DNA deletions and clonal mutations drive premature aging in mitochondrial mutator mice.	Nature Genetics	40	4	392-4	34.284
11	2008	Loeb, L.A. *et al.*	Cancers exhibit a mutator phenotype: clinical implications.	Cancer Research	68	10	3551-7	7.543

13	2007	Vermulst, M. *et al.*	Mitochondrial point mutations do not limit the natural lifespan of mice.	Nature Genetics	39	4	540-3	34.284
14	2007	Zheng, L. *et al.*	Fen1 mutations result in autoimmunity, chronic inflammation and cancers.	Nature Medicine	13	7	812-9	27.136
15	2006	Venkatesan, R.N. *et al.*	Generation of mutator mutants during carcinogenesis	Dna Repair	5	3	95-7	4.199
16	2006	Bielas, J.H. *et al.*	Human cancers express a mutator phenotype.	Proceeding of the National Academy of Sciences of the USA	103	48	18238-42	9.432
17	2005	Bielas, J.H. & Loeb, L.A.	Quantification of random genomic mutations	Nature Methods	2		285-90	16.874

Papers citing the RMC method:

	Year of Publication	Author	Article	Journal	Volume	Issue	Page No.	Impact Factor (JCR 2009)
1	2010	Perzzi, B. *et al.*	The use of PIG-A as a sentinel gene for the study of the somatic mutation rate and of mutagenic agents in vivo	Mutation Research	705	1	pp 3-10	7.097
2	2010	Salk, J.J. *et al.*	Mutational Heterogeneity in Human Cancers: Origin and Consequences	Annual Reviews of Pathology Mechanism	5		51-75	13.5
3	2009	Poovathingal, S.K. *et al.*	Stochastic Drift in Mitochondrial DNA Point Mutations: A Novel Perspective Ex Silico	PLOS Computational Biology	5	11	e1000572	5.759
4	2009	Milbury, C.A. *et al.*	PCR-Based Methods for the Enrichment of Minority Alleles and Mutations	Clinical Chemistry	55	4	632-40	6.263
5	2009	Khrapko, K.	Mitochondrial DNA mutations and aging: devils in the details?	Trends In Genetics	25	2	91-98	8.689
6	2009	Martin, G.M. *et al.*	Aging and Cancer: Two Sides of the Same Coin?	Journals Of Gerontology Series -A Biological Sciences and Medical Sciences	64	6	615-17	3.083
7	2009	Edgar, D & Trifunovic, A.	The mtDNA mutator mouse: Dissecting mitochondrial involvement in aging.	Aging	1	12	1028-32	
8	2009	Gruber, J. *et al.*	The mitochondrial free radical theory of ageing - Where do we stand?	Frontiers in Biosciences	13		6554-79	3.603
9	2008	Kujoth, G.C. *et al.*	Evolving insight into the role of mitochondrial DNA mutations in aging	Experimental Gerontology	43	1	20-23	3.342
10	2008	Kraytsberg, Y. *et al.*	Single molecule PCR in mtDNA mutational analysis: Genuine mutations vs. damage bypass-derived artifacts.	Methods	46	4	269-73	3.763
11	2008	Salvioli, S. *et al.*	The impact of mitochondrial DNA on human lifespan: a view from studies on centenarians.	Biotechnology Journal	3	6	740-9	3.146

12	2007	Garcia, A.M. *et al.*	A model system for analyzing somatic mutations in Drosophila melanogaster	Nature Methods	4	5	401-403	16.874
13	2007	Khrapko, K.	Mitochondrial DNA mutations and aging: a case closed?	Nature Genetics	39	4	445-6	34.284
14	2007	Diehl, F. *et al.*	Digital quantification of mutant DNA in cancer patients	Current Opinion In Oncology	19	1	36-42	4.088
15	2007	Laun, P. *et al.*	Yeast mother cell-specific ageing, genetic (in)stability, and the somatic mutation theory of ageing	Nucleic Acids Research	35	22	7514-26	7.479
16	2007	Kraytsberg, Y. *et al.*	Are somatic mitochondrial DNA mutations relevant to our health? A challenge for mutation analysis techniques	Expert Opinion on Medical Diagnostics	1	1	109-16	4.218
17	2007	Jacinto, F. V. and Esteller, M.	MGMT hypermethylation: A prognostic foe, a predictive friend	DNA repair	6	8	1155-60	4.293
18	2006	Smilenov, L.B.	Tumor development: Haploinsufficiency and local network assembly	Cancer Letters	240	1	17-28	3.741
19	2006	Li, M. *et al.*	BEAMing up for detection and quantification of rare sequence variants	Nature Methods	3	2	95-7	16.874
20	2006	Klein, C.A.	Random mutations, selected mutations: A PIN opens the door to new genetic landscapes	Proceedings Of The National Academy Of Sciences Of The United States Of America	103	48	18033-34	9.432
21	2005	Beckman, R.A. & Loeb, L.A.	Negative clonal selection in tumor evolution	Genetics	171	4	2123-31	3.889